



HAL
open science

Unconventional Hall effect in oriented $\text{Ca}_3\text{Co}_4\text{O}_9$ thin films

H. W. Eng, P. Limelette, W. Prellier, Ch. Simon, R. Fresard

► **To cite this version:**

H. W. Eng, P. Limelette, W. Prellier, Ch. Simon, R. Fresard. Unconventional Hall effect in oriented $\text{Ca}_3\text{Co}_4\text{O}_9$ thin films. *Physical Review B: Condensed Matter and Materials Physics* (1998-2015), 2006, 73 (3), pp.033403. 10.1103/PhysRevB.73.033403 . hal-01870055

HAL Id: hal-01870055

<https://univ-tours.hal.science/hal-01870055>

Submitted on 7 Sep 2018

HAL is a multi-disciplinary open access archive for the deposit and dissemination of scientific research documents, whether they are published or not. The documents may come from teaching and research institutions in France or abroad, or from public or private research centers.

L'archive ouverte pluridisciplinaire **HAL**, est destinée au dépôt et à la diffusion de documents scientifiques de niveau recherche, publiés ou non, émanant des établissements d'enseignement et de recherche français ou étrangers, des laboratoires publics ou privés.

Unconventional Hall effect in oriented $\text{Ca}_3\text{Co}_4\text{O}_9$ thin films

H. W. Eng,¹ P. Limelette,^{2,*} W. Prellier,^{1,†} Ch. Simon,¹ and R. Frésard¹

¹Laboratoire CRISMAT, UMR 6508 CNRS, ENSICAEN, 6, Boulevard du Maréchal Juin, 14050 CAEN Cedex, France

²Groupe Matière Condensée et Matériaux, UMR CNRS 6626, Université de Rennes I, 35042 Rennes, France

(Received 14 April 2005; revised manuscript received 21 September 2005; published 11 January 2006)

Transport properties of the good thermoelectric misfit oxide $\text{Ca}_3\text{Co}_4\text{O}_9$ are examined. In-plane resistivity and Hall resistance measurements were made on epitaxial thin films which were grown on *c*-cut sapphire substrates using the pulsed laser deposition technique. Interpretation of the in-plane transport experiments relates the substrate-induced strain in the resulting film to single crystals under very high pressure (~ 5.5 GPa) consistent with a key role of strong electronic correlation. They are confirmed by the measured high temperature maxima in both resistivity and Hall resistance. While holelike charge carriers are inferred from the Hall effect measurements over the whole investigated temperature range, the Hall resistance reveals a nonmonotonic behavior at low temperatures that could be interpreted with an anomalous contribution. The resulting unconventional temperature dependence of the Hall resistance seems thus to combine high temperature strongly correlated features above 340 K and an anomalous Hall effect at low temperature, below 100 K.

DOI: 10.1103/PhysRevB.73.033403

PACS number(s): 81.15.Fg, 73.50.Jt, 73.50.-h, 73.50.Lw

Good thermoelectric materials,^{1,2} which convert heat into electricity and vice versa, should have high figures of merit (ZT) where $ZT = S^2 T / \rho \kappa$, so S (the thermoelectric power or the Seebeck coefficient) should be large while ρ (resistivity) and κ (thermal conductivity) should be small at a temperature T . In addition to these properties, these materials should be physically and chemically robust for high temperature processes such as the generation of energy from waste heat, and therefore, oxides such as Na_xCoO_2 and $\text{Ca}_3\text{Co}_4\text{O}_9$ have recently received considerable attention.^{3,4} Among the oxides, $\text{Ca}_3\text{Co}_4\text{O}_9$ is very promising because of its high room temperature (RT) thermopower ($125 \mu\text{V}/\text{K}$), low resistivity ($12 \text{ m}\Omega \text{ cm}$), low thermal conductivity [$30 \text{ mW}(\text{cm K})^{-1}$], and resistance to humidity.^{4,5}

$\text{Ca}_3\text{Co}_4\text{O}_9$ is a misfit oxide and can be denoted as $[\text{Ca}_2\text{CoO}_3]^{RS}[\text{CoO}_2]_{1.62}$ to recognize the incommensurate nature of the structure. The structure is composed of alternating layers of a distorted Ca_2CoO_3 rock-salt-like layer (RS) and a CoO_2 cadmium iodide-like layer which are stacked in the *c* axis direction. Crystallographically, these two layers have similar *a*, *c*, and β lattice parameters but different *b* lattice parameters. The ratio of the *b* parameters for the Ca_2CoO_3 layer to CoO_2 layer is 1.62. The material's anisotropic behavior is easily seen through the comparison of the in-plane and out-of-plane resistivity behavior (metallic versus semiconducting, respectively).⁴ Thus, to attain the highest properties in a thermoelectric device, growth along the *c* axis would be best to ensure uniform properties. The bulk can be magnetically aligned along the *c* axis at a high temperature,^{6,7} but the thin film forms provide a more convenient method for manufacturing useful thermoelectric devices. For this reason, we have undertaken the synthesis of $\text{Ca}_3\text{Co}_4\text{O}_9$ films on Al_2O_3 (*c*-cut sapphire) substrates.⁸ The resulting epitaxial film has thermoelectric properties very close to the single crystal ($110 \mu\text{V K}^{-1}$ at RT) but with slightly higher resistivity values (varying from 11 to 21 $\text{m}\Omega \text{ cm}$).

The underlying theory behind the good thermoelectric values for $\text{Ca}_3\text{Co}_4\text{O}_9$ is still not completely understood de-

spite the electronic structures having been studied,⁹ thus more experimental data are needed. From a fundamental aspect, the good properties of the cobaltites ($\text{Ca}_3\text{Co}_4\text{O}_9$ and Na_xCoO_2) are not expected because conventional theory states that carrier concentration should oppositely affect conductivity and thermoelectric power, e.g., high carrier concentrations should lead to high conductivity and low thermoelectric power.¹ High-resolution photoemission spectroscopy has been used to demonstrate that the high thermoelectric power and low conductivity depend upon a narrow conduction band derived from the two-dimensional CoO_2 layers in the structures of $\text{Ca}_3\text{Co}_4\text{O}_9$, $\text{Bi}_2\text{Sr}_2\text{Co}_2\text{O}_9$, and Na_xCoO_2 .¹⁰ Furthermore, transport properties in $\text{Ca}_3\text{Co}_4\text{O}_9$ single crystals were found to display typical features of strongly correlated electron materials.¹¹

Viewing these results, it is interesting to study the transport and Hall effect measurements of $\text{Ca}_3\text{Co}_4\text{O}_9$ made in the form of thin films, and our results are reported in this paper. We are studying the properties of thin films for two reasons: (1) the resulting thin film is strongly oriented in contrast to bulk ceramic, allowing a clear assessment of the anisotropic properties; (2) thin films allow a thorough and rapid examination of the transport properties, in particular the Hall effect properties which can give important information on the conduction mechanisms and the nature of the carriers. Unfortunately Hall effect experiments are generically difficult with single crystals but can be much more easily performed with thin films.

Thin films of $\text{Ca}_3\text{Co}_4\text{O}_9$ were grown on polished *c*-cut (0001-cut) sapphire substrates using a pulsed-laser deposition technique.¹² A black, sintered $\text{Ca}_3\text{Co}_4\text{O}_9$ target was synthesized using conventional solid state techniques,⁴ and a KrF excimer laser beam (Lambda Physik Compex, $\lambda = 248 \text{ nm}$, repetition rate = 3 Hz) was used to deposit the material composition of the target onto the sapphire substrate at the proper deposition conditions (600°C , 0.1 mbar O_2 pressure, and a fluence of 1.7 J cm^{-2}). For more details of the optimization and growth conditions see Ref. 8 The x-ray diffraction of the resulting films, attesting to their good quality and good epitaxial relation with the substrate, was shown

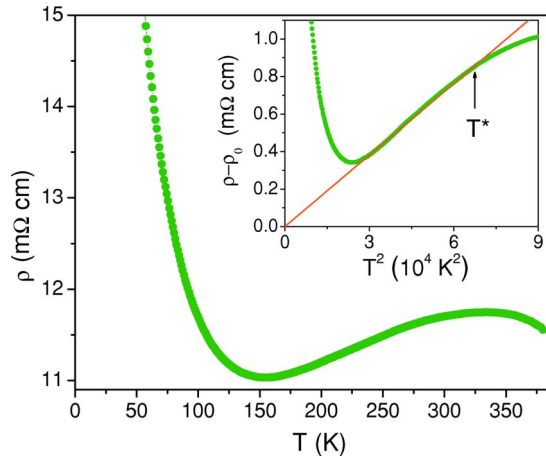


FIG. 1. (Color online) Longitudinal resistivity of a representative $\text{Ca}_3\text{Co}_4\text{O}_9$ thin film. The inset displays the temperature region where $\rho - \rho_0$ versus T^2 is linear. T^* notes a crossover above which the resistivity no longer varies as T^2 .

previously.⁸ A DekTak³ST surface profiler found the thickness of the thin films to be 1800 Å.

The transport measurements were performed using a Quantum Design Physical Property Measurement System (PPMS). The standard four-point probe method was used to measure resistivity, or more specifically, longitudinal resistivity (ρ_{xx}). To make the appropriate connections onto the film, four silver plots were first deposited via thermal evaporation onto the film, and then thin aluminum contact wires were used to connect the areas to the electrodes. For Hall effect measurements, a silver layer and then a gold layer were deposited onto the surface of the film before standard ultraviolet photolithography and argon ion etching were used to pattern microbridges (where the largest widths were 100 μm). The silver layer was deposited via thermal evaporation, and the gold layer was deposited via the rf sputtering technique. The resistivity results, shown in Fig. 1, are similar in behavior to the c axis aligned transport properties of the bulk.^{6,7} There are three interesting regions to note in Fig. 1: below 160 K where the resistivity increases monotonically as temperature T decreases, between 160 and 340 K where the resistivity is metalliclike, and above 340 K where the resistivity decreases as T increases.

It is appealing to analyze the low temperature resistivity using an activation behavior, with an activation temperature T_0 since, below $T_{inc} = 100$ K, muon spin spectroscopy experiments showed the existence of a short-range incommensurate magnetic order in bulk samples.¹³ For sample No. 1, we find $T_0 = 13$ K. Since $T_0 \ll T_{inc}$, our low temperature resistivity data cannot be interpreted in the framework of an activation law, and they require further investigations.

Additionally, two noticeable differences from the bulk are (a) higher resistivity values and (b) a more shallow minima. A possible reason for the increased resistivity can be an increase in grain boundaries in the film, as is commonly seen in many thin metal films.¹⁴ Previous bulk studies^{6,15} have found that oxygen deficiency increased both the resistivity and the thermoelectric power. But oxygen defects are unlikely to be the predominant source of the higher resistivity

TABLE I. The residual resistivities (ρ_0), Fermi liquid transport coefficients (A), and the transport crossover temperatures (T^*) for three thin films made at similar deposition conditions (600 °C, 0.1 mbar O_2 pressure, and a fluence of 1.7 J cm^{-2}) on c -cut sapphire substrates.

Sample	ρ_0 (mΩ cm)	A (10^{-5} mΩ cm K^{-2})	T^* (K)
1	10.65	1.27	240
2	10.69	1.02	231
3	20.93	1.14	240

values because our films showed only an increase in resistivity and not in thermoelectric power.

In bulk samples, a small anomaly of the resistivity has been observed at 380 K,^{4,11,12} and interpreted as a spin state transition.¹⁶ It is not observed here.

In agreement with a previous paper devoted to pressure effects in bulk samples¹¹ the metallic portion of the transport curve is consistent with a Fermi liquid regime, from nearly 160 K up to a characteristic temperature $T^* \sim 240$ K, with a resistivity varying as $\rho = \rho_0 + AT^2$. The first term, ρ_0 , is the residual resistivity and depends on extrinsic factors such as scattering at the grain boundaries. As can be seen in Table I, the values of ρ_0 vary even under similar growth conditions. The second term depends on intrinsic effects and is representative of the strength of the electronic correlations. Strongly enhanced in the vicinity of a Mott Metal-Insulator transition,¹⁷ the high values of the A coefficients listed in Table I (from 1.02 to 1.27×10^{-5} mΩ cm K^{-2}) are rather sample independent and imply strong interactions between electrons.

By comparing in Fig. 2 the pressure dependences of single crystal transport properties¹¹ with the deduced ones

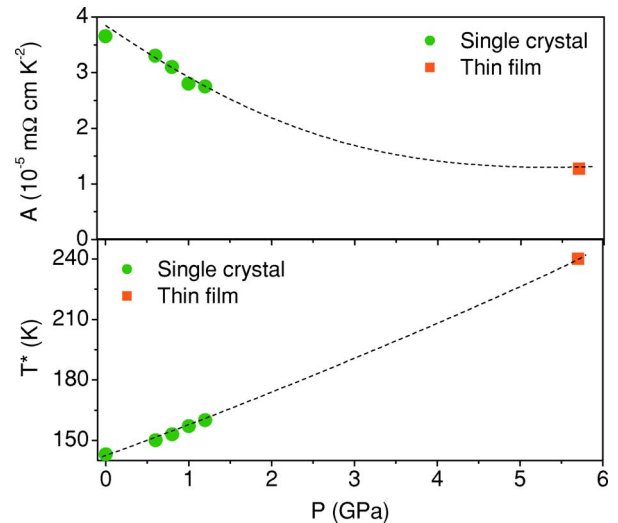


FIG. 2. (Color online) Single crystal (circles) and extrapolated thin film (squares) values for the coefficients of the metallic resistivity as a function of pressure: A , the Fermi liquid transport coefficient (upper panel) and T^* , the transport crossover temperature (lower panel). The strain-induced pressure was extrapolated from the values of T^* . The two dotted lines are guides to the eyes.

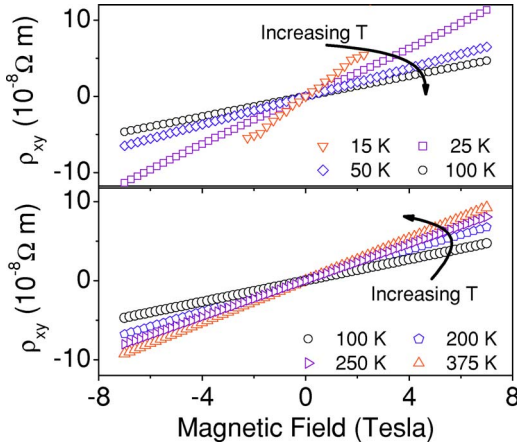


FIG. 3. (Color online) Hall effect measurements of the $\text{Ca}_3\text{Co}_4\text{O}_9$ thin films. The transverse resistivity (ρ_{xy}) versus magnetic field is shown for values above 100 K (upper panel) and below 100 K (lower panel).

for the studied thin film, a lower value of the coefficient A is observed in the thin films suggesting lower correlations. The transport crossover temperature $T^* \sim 240$ K that ends the quadratic Fermi liquid regime is found to be higher than in single crystals in agreement with a lower coefficient A . Consistently, one must emphasize that the product $A(T^*)^2/b_2$, with b_2 the in-plane lattice parameter in the CoO_2 layer,⁴ is of the order of h/e^2 as expected in a Fermi liquid.¹⁷ Indeed, the Fermi liquid transport coefficient A is proportional to the square of the electronic effective mass m^* while the transport crossover temperature T^* represents an effective Fermi temperature, namely renormalized by correlations as $T^* = T_F/m^*$. Thus, the product $A(T^*)^2$ remains independent of the electronic correlations as observed experimentally in both thin films and single crystals by varying pressure.¹¹

From an extrapolation of the single crystal data, the film's T^* yields an approximate strain-induced pressure of approximately 5.5 GPa (Fig. 2). This relatively high pressure extrapolation is not surprising since the in-plane structural parameter of the film, assumed to be equal to the parameter of the substrate in such epitaxial films, is smaller by a few percents than the parameter of the single crystal and roughly corresponds to such a pressure.

This strain effect makes possible to grow as thin film metastable phases (e.g., infinite layers¹⁸ and oxycarbonate superconductors¹⁹) as those synthesized using the high pressure processes.^{20,21} It should be pointed out here that the induced pressure is biaxial, in contrast to what is obtained in the case of hydrostatic pressure already published. In addition, it is well known in these systems that there exists a relaxation of the strains along the thickness which can also broaden the whole result.

Hall effect measurements of the thin films are shown in Fig. 3. [The Hall resistance is equal to the transverse resistivity divided by the magnetic field (ρ_{xy}/H) which is related to the applied magnetic field H .] First of all, let us mention that the positive slope of the Hall resistance implies holelike charge carriers as inferred from thermoelectric power measurements.⁴ Moreover, while in a regular metal the Hall resistance would be nearly temperature independent, Fig. 4

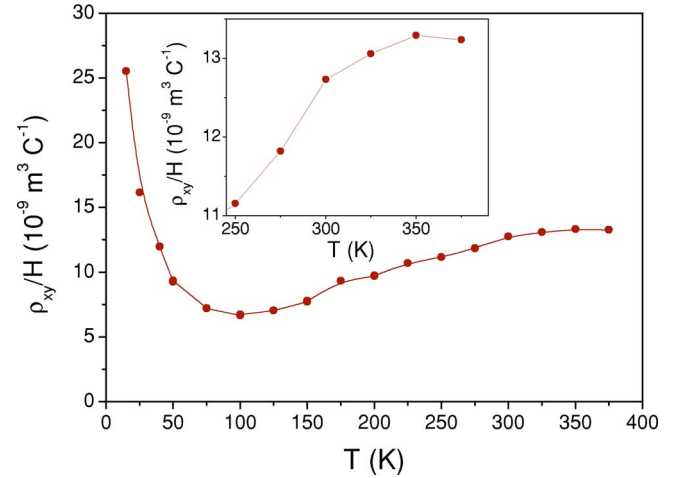


FIG. 4. (Color online) Temperature dependence of the Hall resistance (ρ_{xy}/H). A broad maximum is observed at high temperatures (inset).

exhibits an unconventional temperature dependence with a highly nonmonotonic behavior. In particular, one observes a sizeable increase from 100 K up to 350 K followed by a broad maximum at high temperatures displayed in the inset of Fig. 4. It is inconsistent with the linear increase of the Hall coefficient predicted in the charge frustration scenario.²²

Expected within the framework of the Dynamical Mean-Field Theory (DMFT) of strongly correlated systems,¹⁷ the maxima in both resistivity and Hall resistance result from a strong temperature dependence of the density of states leading to a pseudo gap above T^* . Let us mention that this unusual behavior has already been observed in the strongly correlated quasi-two-dimensional (2D) organic superconductors, $[\beta\text{-(BEDT-TTF)}_2\text{I}_3]$.²³ In addition, even assuming a constant value in this range, the classical analysis drives to unrealistic results. Indeed, the corresponding number of carriers n is estimated to be 5×10^{26} carriers m^{-3} by the inverse relationship to the Hall effect coefficient which is used for common metals ($R_H = 1/ne$). Thus, these results firmly suggest that the observed strong temperature dependence of the Hall resistance including the broad maximum originates from the strong electronic correlations.

Let us now discuss the Hall resistance increase at low temperature. As displayed in Fig. 5, ρ_{xy}/H varies linearly with the inverse temperature below 100 K as $\rho_{xy}/H = 2.6 \times 10^{-9}(1 + 132/T)$. In order to analyze this behavior, the latter relation must be compared to the expression $\rho_{xy}/H = R_H + [(1-N)R_H + R_S]M/H$, where N is the shape of the sample, R_H the ordinary Hall coefficient, R_S the anomalous Hall coefficient²⁴ which originates from spin-orbit effects, and M the magnetization.^{25,26}

Since unfortunately we were not able to measure the magnetization in the film because of the high contribution of the substrate, let us consider the bulk one.

This can be estimated to be of Curie type with a Curie constant C_0 of the order of 0.12 K,⁴ that should be related to the transverse resistivity following Eq. (1),

$$\rho_{xy}/H \approx R_H[1 + (1 + R_S/R_H)C_0/T]. \quad (1)$$

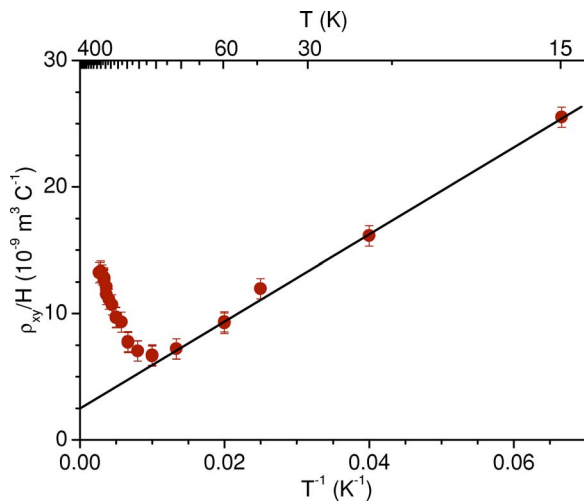


FIG. 5. (Color online) The Hall resistance (ρ_{xy}/H) values of the thin film versus inverse temperature. A linear relationship is observed below 100 K as $\rho_{xy}/H = 2.6 \times 10^{-9}(1 + 132/T)$.

Thus, by comparing the experimental relation with Eq. (1), one deduces a strong anomalous component as $R_S/R_H > 10^3$. Even if a quantitative analysis of R_S would require magnetization measurements in the films as a function of temperature, its order of magnitude compared to R_H testifies unambiguously to this anomalous component.

Furthermore, since the ordinary Hall coefficient is expected to be weakly temperature dependent at low temperature, the experimental relation [of Eq. (1)] gives also an estimate of $R_H \approx 2.6 \times 10^{-9} \text{ m}^3 \text{ C}^{-1}$ (see Fig. 5). Because in this limit the ordinary Hall coefficient is independent of the electronic correlations,¹⁷ this value leads to a reasonable holelike charge carriers density $n \approx 2.4 \times 10^{+27} \text{ m}^{-3}$ with $R_H = 1/ne$.

Interestingly, the latter density corresponds to a unit cell volume $V \approx 1.48 \times 10^{-28} \text{ m}^{-3}$ to a hole doping of the order of 0.36 per cobalt of the CoO_2 layer. Assuming an insulating rock-salt-like layer, this doping is consistent with a crude estimation inferred from the electroneutrality in the $[\text{Ca}_2\text{CoO}_3]_{0.62}^{\text{RS}}[\text{CoO}_2]$. Thus, it could suggest that the transport properties are essentially governed by itinerant holes in the CoO_2 layers.

In summary the in-plane resistivity and Hall effect measurements made on epitaxial thin films of $\text{Ca}_3\text{Co}_4\text{O}_9$ grown on *c*-cut sapphire substrates confirmed the strong electron correlations. In the thin film form, the in-plane transport properties verified that the strain from the substrate can be related to very high pressures (~ 5.5 GPa) in single crystals. By using the strain induced by the substrate as an equivalent pressure, we have shown that the effective mass of the charge carriers can be significantly modified. The strong electron correlation nature is borne out in the high temperature Hall effect measurements where the observed Hall resistance plateaus and no longer follows expected Fermi liquid behavior. Finally at low temperatures, the observed high Hall resistances may be attributed to an anomalous Hall effect and should be related to the magnetic susceptibility as well as the appearance of the short-range IC spin-density-wave order. The misfit nature of $\text{Ca}_3\text{Co}_4\text{O}_9$ effectively localizes the itinerant holes in the CoO_2 layers, leading to a narrow conduction band that yields strongly correlated transport properties.

The funding for this project was provided by the Centre National de la Recherche Scientifique (CNRS) and the Conseil Régional de Basse-Normandie. We would also like to thank Dr. L. Méchin for patterning the microbridges on the thin films and Professor B. Mercey, Dr. M. Singh, and Dr. P. Padhan for helpful discussions.

*Present address: Laboratoire LEMA, UMR 6517 CNRS-CEA, Université Rabelais, UFR Sciences, Parc de Grandmont, 37200 Tours, France.

†Electronic address: prellier@ensicaen.fr

¹G. Mahan, B. Sales, and J. Sharp, *Phys. Today* **50**, 42 (1997).

²F. Disalvo, *Science* **285**, 703 (1999).

³I. Terasaki, Y. Sasago, and K. Uchinokura, *Phys. Rev. B* **56**, R12685 (1997).

⁴A. C. Masset *et al.*, *Phys. Rev. B* **62**, 166 (2000).

⁵A. Satake, H. Tanaka, T. Ohkawa, T. Fujii, and I. Terasaki, *J. Appl. Phys.* **96**, 931 (2004).

⁶M. Sano, S. Horii, I. Matsubara, R. Funahashi, M. Shikano, and J. I. Shimoyama, *J. Appl. Phys.* **42**, L198 (2003).

⁷S. Horii *et al.*, *Jpn. J. Appl. Phys., Part 1* **42**, 7018 (2003).

⁸H. Eng, W. Prellier, S. Hébert, D. Grebille, L. Méchin, and B. Mercey, *J. Appl. Phys.* **97**, 013706 (2005).

⁹R. Asahi, J. Sugiyama, and T. Tani, *Phys. Rev. B* **66**, 155103 (2002).

¹⁰T. Takeuchi *et al.*, *Phys. Rev. B* **69**, 125410 (2004).

¹¹P. Limelette *et al.*, *Phys. Rev. B* **71**, 233108 (2005).

¹²W. Prellier, A. Haghiri-Gosnet, B. Mercey, P. Lecoeur, M. Hervieu, C. Simon, and B. Raveau, *Appl. Phys. Lett.* **77**, 1023 (2000).

¹³M. Muller, T. Vekua, and H. J. Mikeska, *Phys. Rev. B* **66**, 134423 (2002).

¹⁴S. Kasap, *Principles of Electrical Engineering Materials and Devices* (McGraw-Hill, New York, 2002) pp. 141–142.

¹⁵M. Karppinen, H. Fjellvag, T. Konno, Y. Morita, T. Motohashi, and H. Yamauchi, *Chem. Mater.* **16**, 2790 (2004).

¹⁶J. Sugiyama, C. Xia, and T. Tani, *Phys. Rev. B* **67**, 104410 (2003).

¹⁷A. Georges, G. Kotliar, W. Krauth, and M. Rozenberg, *Rev. Mod. Phys.* **68**, 13 (1996).

¹⁸D. Norton, B. Chakoumatos, J. Budai, D. Lowdes, B. Sales, J. Thompson, and D. Christen, *Science* **265**, 2074 (1994).

¹⁹J. Allen, B. Mercey, W. Prellier, J. Hamet, M. Hervieu, and B. Raveau, *Physica C* **241**, 158 (1995).

²⁰Z. Hiroi and M. Takano, *Physica C* **29**, 235 (1994).

²¹M. Alario-Franco, *et al.*, *Physica C* **231**, 103 (1994).

²²O. I. Motrunich and P. A. Lee, *Phys. Rev. B* **69**, 214516 (2004).

²³B. Korin-Hamzić, L. Forró, and J. R. Cooper, *Phys. Rev. B* **41**, R11646 (1990).

²⁴C. Hurd, *The Hall Effect in Metals and Alloys* (Plenum Press: New York, 1972).

²⁵J. Luttinger, *Phys. Rev.* **112**, 739 (1958).

²⁶P. Nozières and C. Lewiner, *J. Phys. (Paris)* **34**, 901 (1973).